

Energetics of CO on stepped and kinked Cu surfaces: A comparative theoretical studyFaisal Mehmood,¹ Abdelkader Kara,^{1,2} Talat S. Rahman,^{1,2} and Klaus Peter Bohnen³¹*Department of Physics, 116 Cardwell Hall, Kansas State University, Manhattan, Kansas 66506-2600, USA*²*Department of Physics, University of Central Florida, 4000 Central Florida Boulevard, Orlando, Florida 32816-2385, USA*³*Forschungszentrum Karlsruhe, Institut für Festkörperphysik, D-76021 Karlsruhe, Germany*

(Received 12 December 2005; published 30 October 2006)

Our *ab initio* calculations of CO adsorption on several low and high Miller index surfaces of Cu show that the adsorption energy increases as the coordination of the adsorption site decreases from 9 to 6, in qualitative agreement with experimental observations. On each surface the adsorption energy is also found to decrease with increase in coverage, although the decrement is not uniform. Calculated vibrational properties show an increase in the frequency of the metal-C mode with decrease in coordination, but no such effect is found for the frequency of the CO stretch mode. Examination of the surface electronic structure shows CO adsorption to have a strong effect on the local density of state of the substrate atoms. We also report calculated energetics of CO diffusion on Cu(111) and Cu(211).

DOI: [10.1103/PhysRevB.74.155439](https://doi.org/10.1103/PhysRevB.74.155439)

PACS number(s): 73.20.-r

I. INTRODUCTION

Investigation of CO adsorption on well-defined transition-metal surfaces has been of great academic interest for several decades.¹⁻⁷ Because of the molecule's obvious relevance to many industrial processes, it has served as a prototype reactant in studies aiming to provide an understanding of catalytic reactions.³⁻⁵ Through examination of adsorption and desorption energies and sticking coefficients,³⁻⁵ experimental and theoretical studies^{6,7} have attempted to identify the "active sites" for chemical reactions. However, since real catalysts consist of small metal clusters with microfacets of various orientations, attention has turned from low Miller index surfaces to those with defects like steps and kinks which may play a specific role in determining surface reactivity.⁸ A plausible way to understand systematically the effect of steps and kinks on chemisorption was provided in a recent thermal deposition spectroscopy (TDS) study which undertook the examination of CO adsorption on a set of vicinal surfaces. A dependence of the CO binding energy on the coordination of the adsorption site was found, but surprisingly the effect did not extend to the least undercoordinated sites, namely that of CO on the kink sites of Cu(532). Instead Vollmer *et al.*⁹ find hardly any difference in the adsorption energy for CO on a step and a kink site atom implying that coordination alone may not account for the adsorption energy on this vicinal surface. As proposed by Bagus and Wöll¹⁰ in their theoretical study of CO adsorption on Cu(100), the repulsive interaction between the O atom and the *s* states of the substrate can also play an important role in determining the trends in the adsorption energy. Similarly in an extensive first-principles^{11,12} study of CO adsorption on the (111) surface of several transition metals, Gajdos *et al.*¹³ argue that the details of the adsorption kinetics may be controlled by the extent of the shift of the 4σ and 5σ orbital charge density from the C-O bond to the region below the carbon (metal surface). Of course application of methods based on density-functional theory (DFT) may raise some concerns since on the low Miller index surfaces of Cu they (i) show preference for the hollow site,¹⁴ while the analysis of experimental data point to

preference for the top site,⁹ (ii) overestimate CO adsorption energy^{13,14} by about 0.2 eV as compared to experimental data. Very recently several groups¹⁴⁻¹⁶ have attempted to supplement DFT functionals in various ways so as to remedy the above shortcomings for this system with some success. Our intention in this paper is, however, to carry out a systematic, comparative study of CO chemisorption on the on-top sites of a set of low and high Miller index surfaces of Cu to see the trends in adsorption energies as a function of local coordination and CO coverage. While these calculations have been motivated by experimental data,⁹ we are also aware of theoretical work^{10,13,15} on CO adsorption on a couple of surfaces that we are considering here. Naturally, we will compare our results to all available information that exists to date.

In addition to the trends in CO adsorption energy on Cu surfaces, we are also interested in the diffusion barrier for CO, since this is a necessary step in any chemical reaction involving CO on the surface. A comparative study of the diffusion of CO on Cu(111) and Cu(211) is presented. Also, given the interest in reactions at and near steps and kinks on surfaces, we have calculated CO adsorption energies on several sites near these defects. We are also including in this work the effect of CO adsorption on the atomic relaxations of the substrate vicinal surface, to see how the trends in relaxation patterns correlate with those in the surface electronic structure.

After giving some computational details in the next section, we present in Sec. III an analysis of the calculated CO adsorption energies as a function of local coordination, and their comparison with results from experiments and other calculations. This is followed by investigations of the implication of increasing CO coverage on adsorption energetics and characterization of the changes in the surface electronic structure (local density of states, work functions) on CO adsorption. The vibrational frequencies of CO on the set of Cu surfaces under consideration is also presented. The energetics of diffusion of CO along characteristic paths on Cu(111) and Cu(211) conclude the presentation of our results. Finally conclusions of our work are presented in Sec. IV.

II. COMPUTATIONAL METHODS

Ab initio calculations performed in this study are based on the well-known density-functional theory (DFT).^{11,12} For purposes here, a systematic study of the energetics and the electronic structure of a set of Cu surfaces of varying geometry was made by solving Kohn-Sham equations in a plane-wave basis set using the Vienna *ab initio* simulation package (VASP).¹⁷⁻¹⁹ The electron-ion interactions for C, O, and Cu are described by ultrasoft pseudopotentials proposed by Vanderbilt.²⁰ A plane-wave energy cutoff of 400 eV was used for all calculations and is found to be sufficient for these systems.^{13,21} Additionally, the generalized gradient correction of Perdew and Wang²² (PW91) was used, since it has been shown to give results for adsorption energetics and structural parameters which are in better agreement with experiment as compared to those obtained using the local density approximation (LDA).^{14,23} The calculated bulk lattice constant for Cu was found to be 3.6471 Å and the Brillouin-zone sampling of the total energy was based on the technique devised by Monkhorst and Pack²⁴ for all bulk calculations with a k -point mesh of $10 \times 10 \times 10$.

The supercell approach with periodic boundaries is employed to model the surface systems. To calculate the total energies for several coverages of CO, we have used a surface unit cell consisting of 2–8 atoms per layer. While the definition of the coverage for the low Miller index surfaces is conceptually easy and simply defined as the ratio of the number of adsorbate and substrate atoms in the surface unit cell, for surfaces with steps and kinks we also need to take into account the specific areas of the unit cells, for consistency. For vicinal surfaces we have thus adopted a definition for coverage (θ^{vic}) which is related to the one on the (111) surface (θ) according to $\theta^{\text{vic}} = \theta \frac{A_{(111)}}{A_{\text{vic}}}$, where $A_{(111)}$ is the area of the surface unit cell of Cu(111) and A_{vic} is the area of the vicinal surface. The nearest-neighbor distance 2.579 Å found in our calculations is used for evaluating the area of the surface unit cell.

Cu(100) and Cu(111) surface systems were modeled by a four-layer (16 atoms) tetragonal and hexagonal supercell, respectively, and 11 Å of vacuum. For Cu(100), calculations were performed for a $c(2 \times 2)$ overlayer, corresponding to 50% coverage of CO, and for a (1×1) structure corresponding to full coverage (we are aware that such a high coverage is unrealistic) for comparison. For Cu(111), the $p(2 \times 2)$ structure corresponding to 33% CO coverage, and those corresponding to 66% and 100% coverages were also studied. For all coverages considered on Cu(100) and Cu(111), the CO molecule was taken to be adsorbed on the on-top sites, with the molecule sitting perpendicular to the surface and the C atom forming a bond with the Cu surface, as reported in a number of experiments.^{9,25,26} For proper convergence of the total energy of the system Monkhorst-Pack k -point mesh of $(4 \times 4 \times 1)$ was used for Cu(100) and of $(6 \times 6 \times 1)$ for Cu(111).

The Cu(110), Cu(211), and Cu(221) surfaces were modeled by an orthorhombic supercell of 8, 17, and 22 layers, respectively, separated with approximately 12 Å vacuum. For Cu(110), a (2×1) surface unit cell (16 Cu atoms) with

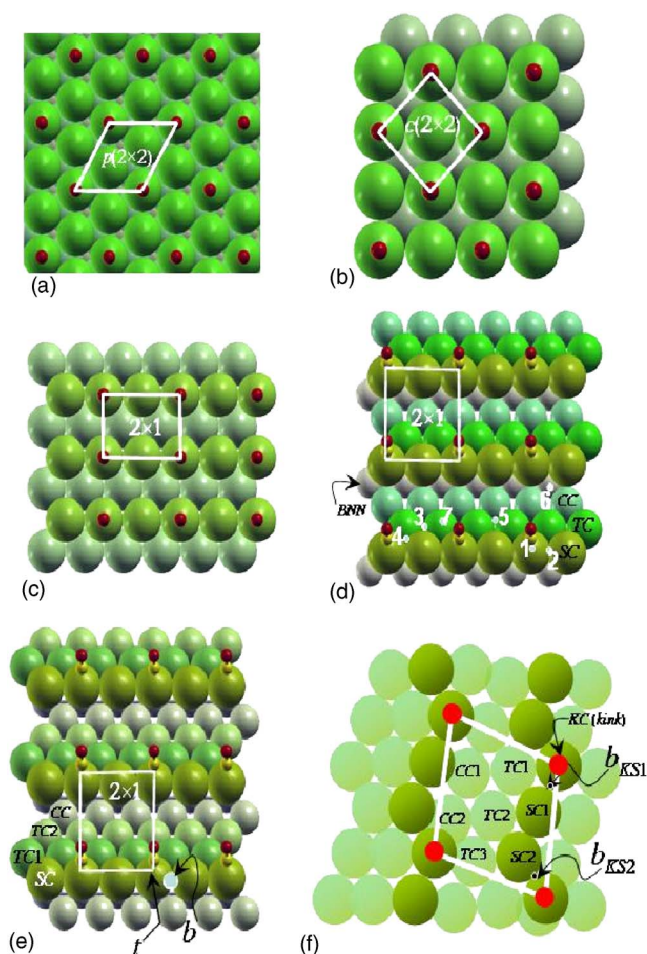


FIG. 1. (Color online) Top view of fcc (a) (111), (b) (100), (c) (110), (d) (211), (e) (221), and (f) (532) surface. The red circles represent the location of CO molecules whose coverages are shown. The lighter the shade of green, the higher is the location of the Cu atom along the surface normal. Note that on the (532) surface all eight atoms are nonequivalent and belong to eight different layers according to the definition of “layers” for the vicinal surfaces.

one (or two) adsorbed CO molecules was chosen to model 50% (or 100%) coverage of CO, as shown in Fig. 1(c). A Monkhorst-Pack k -point mesh of $(5 \times 7 \times 1)$ was used for this surface. Both Cu(211) and Cu(221) being regularly stepped surfaces with monoatomic steps and terrace width of three and four atoms, needed 34 and 44 atoms, respectively, to model a (2×1) surface unit cell. According to the above definition of coverage, the supercell for Cu(211) corresponds to 17.69% coverage, while for Cu(221) the corresponding coverage is 14.44%. Calculations for twice the coverage were also performed by incorporating an additional CO molecule in the same supercell. The detailed analysis was performed for the on-top and the bridge site on Cu(211) and Cu(221). A Monkhorst-Pack k -point mesh of $(5 \times 4 \times 1)$ was used for (211) and $5 \times 3 \times 1$ was used for (211) and (221) surface, respectively. Finally, Cu(532) whose surface consists of regularly spaced kinks, was modeled by a simple monoclinic supercell of five layers, where each layer has eight nonequivalent atoms. These five layers were separated

by 12 Å of vacuum. A Monkhorst-Pack k -point mesh of ($3 \times 4 \times 1$) was used and CO was adsorbed on top of the Cu atom at the kink site, which is the preferred adsorption site from experiments.⁹ Two coverages (10.76% and 21.52%) of CO on Cu(532) were modeled by adsorbing one and two molecules, respectively, on the kink site (and on a site very next to kinked site).

Since vicinal surfaces provide local environments with a range of coordinations, a hierarchy of adsorption sites may exist on them.²⁷ We have carried out calculations for one of the stepped surfaces, Cu(211), for eight different sites which are labeled in Fig. 1(d), as we shall see, the results point to a preference for the bridge site, for Cu(221) and Cu(532) we have calculated adsorption energies for the bridge sites, in addition to the on-top site.

In order to calculate the total energy of the system for a relaxed configuration, all atoms in the supercell were allowed to move in all directions and the structures were relaxed until the forces acting on each atom were converged to less than 0.02 eV/Å. Adsorption energy (E_{ad}) was calculated by subtracting the total energy of the CO molecule (E_{CO}) and that of the corresponding fully relaxed clean-Cu surface system (E_{Cu}) from the total energy of CO/Cu surface system: $E_{ad} = E_{CO/Cu} - E_{CO} - E_{Cu}$. Another quantity of interest, the work function, was calculated by taking the difference of the average vacuum potential and Fermi energy for each surface. The finite difference method was used to obtain vibrational frequencies of the CO molecule in the gas phase and on the surfaces. CO internal stretching and CO-metal stretch frequencies were calculated in the direction perpendicular to the surface. To analyze the nature of the bonding between CO and the Cu atoms, local density of states were also obtained. A Gaussian function of 0.2 eV width was used to smoothen the local density of states (LDOS).

III. RESULTS AND DISCUSSION

As already mentioned above, the collection of surfaces studied here provide adsorption sites with coordination ranging from 6 to 9. The kink sites with coordination 6 on Cu(532) are particularly interesting because of their unexpected results from TDS measurements.⁹ Also of significance is the fact that the step edges of Cu(211) and Cu(221) represent the two different microfacets of monoatomic steps on fcc(111) surfaces. Cu(211) has the (100) microfacet while Cu(221) has the (111) microfacet. It will be interesting to see if such differences in the microfacet geometry affect the energetics of CO on these surfaces. In Table I, we have compared our calculated CO bond lengths and the corresponding C-Cu distances for these three surfaces. While d_{C-O} , the C-O bond length, remains insensitive to the local geometry and coordination, d_{C-Cu} , the C-Cu bond length, is much shorter for the bridge (b) site followed by that for the on-top (t) site. As for Cu(532), there are two nonequivalent bridge sites labeled by b_{KS1} and b_{KS2} in Table I and Fig. 1(f). For on-top adsorption on Cu(211), d_{C-O} have already been calculated^{25,26} and our results are in agreement. When CO is adsorbed on the bridge site on the three vicinal surfaces, the

TABLE I. Calculated bond lengths of CO adsorbed on the top (t) and bridge (b) sites on Cu(211), Cu(221), and Cu(532). The two nonequivalent bridge sites on Cu(532) [see Fig. 1(f)] are labeled as b_{KS1} and b_{KS2} . Values in square brackets are reported by others (Ref. 21).

Surface	Bond length (Å)	
	d_{C-O}	d_{C-Cu}
Cu(211)	1.16 (t)[1.154]	1.85 (t)[1.84]
	1.17 (b)[1.168]	1.51 (b)[1.50]
Cu(221)	1.16 (t)	1.86 (t)
	1.17 (b)	1.51 (b)
Cu(532)	1.16 (t)	1.85 (t)
	1.17 (b_{KS1})	1.56 (b_{KS1})
	1.17 (b_{KS2})	1.58 (b_{KS2})

C-O bond length increases slightly and the C-Cu bond decreases. Earlier DFT calculations for CO on Cu(211) also find the same trend.²¹ The only available experimental data²⁸⁻³⁰ for CO bond lengths are for the low Miller index surfaces and are in good agreement with our calculated value of 1.16 Å for d_{C-O} and 1.85 and 1.86 Å for d_{C-Cu} , for Cu(111) and Cu(100), respectively. A small increase of 0.02 Å is found for the C-Cu bond length when the CO coverage is increased from 33% to 100%, whereas when the coverage is doubled from 50% to 100% on Cu(100) and Cu(110), we find only 0.01 Å increase in the C-Cu bond length and no change is found in the C-O bond length.

A. Adsorption energies

Our calculated CO adsorption energies on the above-mentioned Cu surfaces and their surface atomic coordination are summarized in Table II. The lowest coordinated, and in turn the most favorable for CO adsorption, is the kink atom on Cu(532) [Fig. 1(f)], with the highest adsorption energy of 0.98 eV at CO coverage of 10.75% (i.e., one CO molecule per kink atom). The calculated adsorption energy for this case is found to be particularly higher than what has been seen experimentally. Although overestimation of adsorption energies is typical of DFT based calculations, it is expected that the qualitative behavior would be similar. For CO adsorption on the steps of Cu(110), Cu(211), and Cu(221) with atomic coordination 7, our calculations find E_{ad} to be about 0.86 ± 0.01 eV, while experimental values are around 0.6 eV. For adsorption on the kink site we predict an increase in E_{ad} while experiments⁹ find it to be the same as that for the steps. As is clear from Fig. 2 our calculated values scale nicely with surface coordination and the variation is larger than that extracted from experimental data, which is also plotted in Fig. 2 for comparison. We offer here some possible answers to the natural question: why this difference between theory and experiment? For example, there is the possibility that site blocking by another CO could lead to a smaller measured value on an open surface like Cu(532). To test the viability of this proposition, we adsorbed an additional CO

TABLE II. Variation of the adsorption energy (E_{ad}) of CO for two coverages on several Cu surfaces. The coverage in the lower entry (in parentheses) is twice as large as the one for the top entry for each surface. In the upper entries the experimental values from Ref. 9 are in parentheses. N_{NN} is the coordination of the adsorption site.

Surface	Cu(111)	Cu(100)	Cu(110)	Cu(211)	Cu(221)	Cu(532)
N_{NN}	9	8	7	7	7	6
E_{ad} (eV)	0.634 (0.49)	0.77(0.53)	0.87(0.56)	0.86(0.61)	0.85(0.60)	0.98(0.59)
				0.925(<i>b</i>)	0.933(<i>b</i>)	0.941(<i>b</i> _{KS1})
						0.949(<i>b</i> _{KS2})
	0.18(100%)	0.18(100%)	0.55(100%)	0.61(35.4%)	0.65(28.9%)	0.85(21.5%)

molecule on a site next to the kink site [SC1 in Fig. 1(f)] which increased the coverage to 21.5%. As we see in Table II, this leads to a decrease in the adsorption energy to 0.85 eV which is very close to what we find for Cu stepped surfaces. In fact, the variation of the adsorption energy with coverage is quite remarkable for all considered surfaces. For Cu(221), E_{ad} changes from 0.85 eV for 14.5% coverage to 0.65 eV for 29% coverage. Although DFT studies of CO adsorption on Cu(110) and Cu(211) have already been reported in the literature,^{13,15,21,31} for completeness we have included them in Table II. Note that although we have used the same (2×1) cell in the calculations for Cu(211) and Cu(221), the difference in their terrace widths leads to a small difference in the calculated coverage (17.69%) for Cu(211). The same (2×1) cell used for Cu(110) (with [110] and [100], along the x and y axis, respectively), as shown in Fig. 1(c), results in a 50% coverage. The CO molecule is adsorbed on the top site on Cu(110) and Cu(211), as shown in Figs. 1(d) and 1(e). Our calculated adsorption energies are within 20 meV of each other for all cases involving atoms with coordination 7. For Cu(211) our calculated value is somewhat smaller than that in Ref. 13 which may be associated with the differences in computational parameters. For CO adsorption on Cu(110), Liem and Clarke³¹ obtained an

adsorption energy of 0.95 eV for the same coverage and on-top site adsorption. The discrepancy with our results could be due to the usage of fewer layers and smaller k -point mesh and energy cutoff in their calculations. For example, we find the adsorption energy to change from 0.87 to 0.89 eV when we reduce the number of layers in our supercell from 8 to 6 (note that a three-layer slab was used in Ref. 31). Also, we have found an energy cutoff of 300 eV to be not sufficient to provide converged results for the total energy for open surfaces such as the (110). A cutoff of at least 400 eV (the value used in all our calculations) is required for accurate determination of adsorption energies.

For the next surface in this hierarchy, Cu(100), whose surface atoms have coordination 8, we obtain an adsorption energy of 0.77 eV for a 50% CO coverage. This result is again higher than the experimental value which ranges between 0.5 and 0.57 eV.^{9,26,32} On the other hand, our result is in close agreement with the calculated value of 0.863 eV found for a smaller coverage of 0.25 monolayer (ML) by Gajdos and Hafner,¹⁵ using the same DFT technique. Finally, we turn to Cu(111) whose surface atoms with coordination 9 display the lowest adsorption energy of all sites discussed here. For this particular surface, we have used the experimentally studied $p(2 \times 2)$ overlayer which corresponds to 33% CO coverage. For 0.25-ML coverage an adsorption energy of 0.74 eV has already been reported.¹³ The small difference from our result of 0.634 eV may be assigned to the difference in coverage, and is consistent with the argument that adsorption energy decreases with an increase of coverage. The clear trend of increasing adsorption energy with decreasing local coordination can be seen from the plot in Fig. 2 in which solid triangles are our calculated values and empty triangles are the ones from the experiment.⁹

As expected we find a hierarchy of adsorption sites on Cu(211) with E_{ad} ranging from 0.62 to 0.92 eV. The bridge site [labeled 2 in Fig. 1(d)] was found to be slightly preferred over on-top by ~ 0.06 eV. The sites labeled 3 (fcc-hollow) and 4 (hcp hollow near step edge), in Fig. 1(d), were the next preferred with adsorption energies of 0.78 and 0.89 eV, respectively. The least favorable site on this surface was found to be the site labeled 6 which is between two step edges and two corner atoms and has the highest number of bonds with the carbon atom and an adsorption energy of 0.56 eV. On sites 5, 7, and 8 adsorption energies are very close to each other ranging from 0.6 to 0.65 eV. The adsorption site with the highest coordination is the corner atom (CC) on Cu(211)

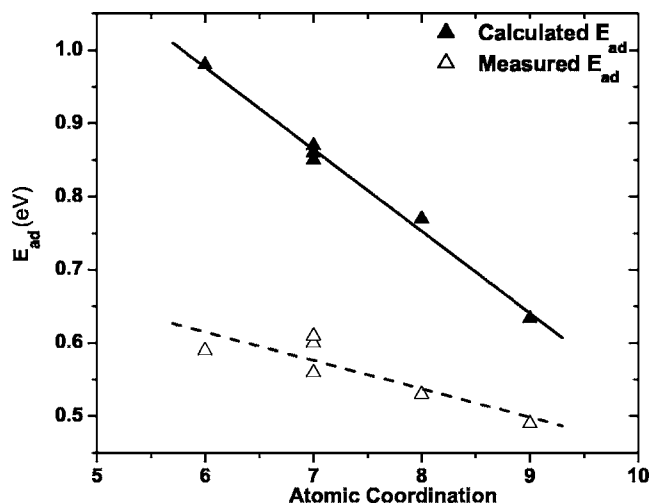


FIG. 2. Plot of adsorption energy vs coordination of the host Cu atom. Solid triangles are calculated values and empty ones are experimental.

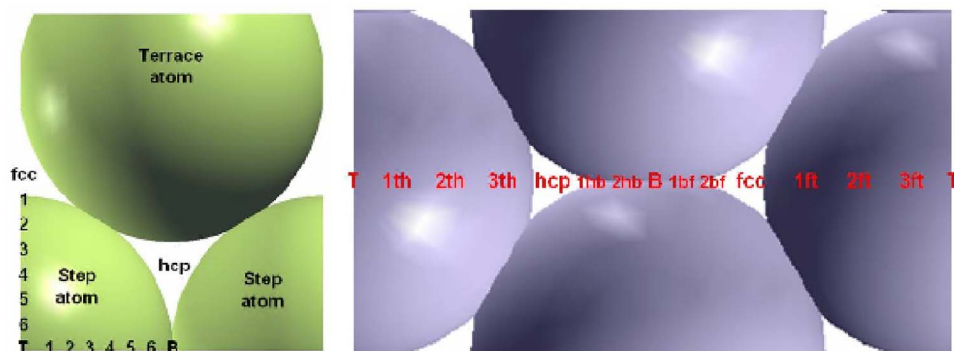


FIG. 3. (Color online) Chosen diffusion path for CO molecule on Cu(111) (on the left) and Cu(211) (on the right).

with effective surface coordination of 10, and labeled as site 8 in Fig. 1(d), for which we find the adsorption energy to be the lowest of all (0.617 eV), consistent with the above discussion. Note that we find the bridge site to be preferred also by about 0.08 eV over the on-top site for CO adsorption on Cu(221). On the other hand, for Cu(532), which has two nonequivalent bridge sites referred to as b_{KS1} and b_{KS2} in Table II and Fig. 1(f), we find the adsorption energy to be 0.94 eV which is less than that on the kink site.

In all cases, adsorption energies drop by 130–250 meV when the coverage is doubled for these high Miller index surfaces. Various experiments already show the strong dependence of adsorption energy on CO coverage on Cu surfaces.^{33–35} Our results are in qualitative agreement with those from electron energy-loss spectroscopy (EELS) experiments of Peterson and Kevan³⁴ which show a 50% decrease in adsorption energy for a 0.3-ML increase in CO coverage for Cu(100).

B. CO diffusion on metal surface

One of the experimental techniques to determine the adsorption energies is the temperature programmed desorption (TPD). It is hence desirable to develop a technique by which TPD spectra are calculated for a given system. For the case of low Miller index surfaces, the task may be trivial as only a limited number of processes are involved. But for the case of real surfaces with steps and kinks, the situation becomes more cumbersome. To achieve a realistic description of the TPD spectra obtained for these surfaces, one needs to calculate not only adsorption energies for the sites with different local environments, but also activation energies associated with different diffusion paths. As we have reported above, the CO molecules adsorb preferably near kinks and steps, and it is hence rarely that CO molecules sit on the down side of the terrace [sites 6 and 8 in Fig. 1(d)]. The relevant energies are hence those associated with diffusion on Cu(111) and near the step of a Cu vicinal surface. Here we have in mind systems dominated by the presence of (111) facets and step edges. The knowledge of these activation energies along with the different adsorption energies will constitute the base for kinetic Monte Carlo simulations that will determine the TPD spectra. With this in mind, the energy landscape for the diffusion of CO on Cu(111) and Cu(211) surfaces were calculated. Since we were interested in describing the motion of the CO molecule between the equilibrium sites, the path on

Cu(111) was chosen to be from one top site to the adjacent one, passing through the fcc hollow, the bridge, and the hcp hollow sites (Fig. 3). Atoms in all layers of the metal surface were allowed to relax fully in all three directions, while the C atom was allowed to do so only in the high-symmetry sites (on-top, bridge, etc.). For the intermediate sites the carbon atom was allowed to move only along the diffusion path and the rest of the system was allowed to relax fully. Three intermediate points between the top and the bridge site and two points each along the bridge–fcc–hollow and bridge–hcp–hollow directions were calculated, as shown in Fig. 4(a). The relative energy profile of the CO molecule on Cu(111) is shown in Fig. 4(a). As in previous studies, our calculations based on DFT with GGA indicate that CO prefers to sit on

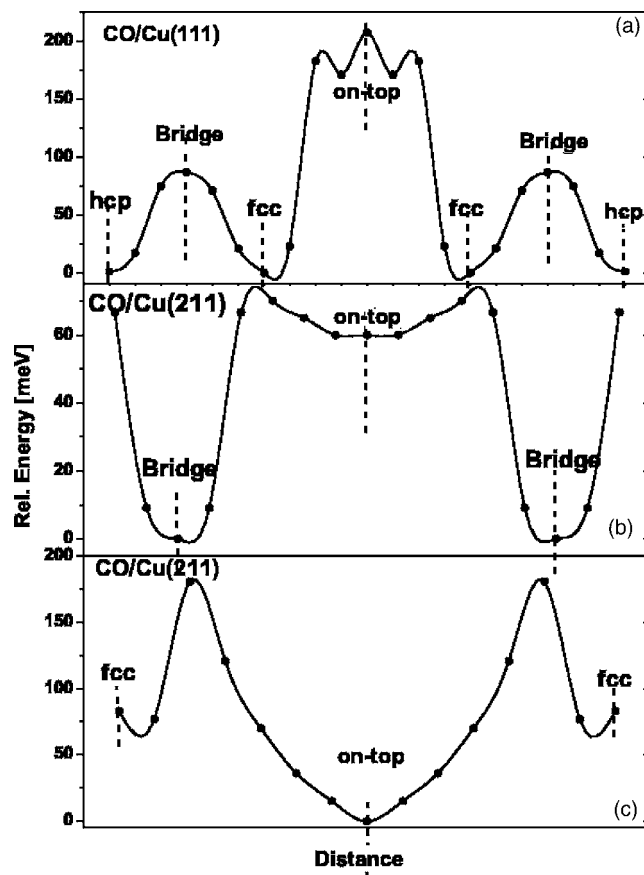


FIG. 4. Calculated energetics for CO along specific diffusion paths on (a) Cu(111); (b) and (c) Cu(211).

TABLE III. Comparison of multilayer relaxations (%) of the clean and CO adsorbed Cu surfaces.

$d_{i,i+1}$	Cu(211)	CO/Cu(211)	Cu(221)	CO/Cu(221)	Cu(532)	CO/Cu(532)
$d_{1,2}$	-15.6	+6.4	-16.5	+2.9	-17.7	+23.5
$d_{2,3}$	-11.4	-15.7	-1.9	-10.2	-18.9	-18.8
$d_{3,4}$	+11.3	+0.2	-15.2	-9.5	-12.7	-16.2
$d_{4,5}$	-4.1	+6.9	+18.8	+6.0	-15.0	-12.0
$d_{5,6}$	-2.0	-3.9	-2.9	+3.8	-15.0	-16.6
$d_{6,7}$	+2.0	-1.8	-6.1	-2.7	-1.4	-3.9
$d_{7,8}$	-2.1	+1.8	+2.5	+2.0	+1.9	-5.2
$d_{8,9}$	+0.1	-0.6	+2.3	-4.4	+25.0	+16.4
$d_{9,10}$			-0.9	+2.2	-9.7	+9.6
$d_{10,11}$			+2.0	+1.0	-2.9	-6.6
$d_{11,12}$			+0.8	-1.1	-4.7	-5.4
$d_{12,13}$				-0.1	-2.0	-0.6
$d_{13,14}$					+0.2	-3.3
$d_{14,15}$					-1.1	-2.9
$d_{15,16}$					+0.1	+3.7
$d_{16,17}$					+1.1	-4.2
$d_{17,18}$					-1.8	+2.3
$d_{18,19}$					-1.6	-4.8
$d_{19,20}$					-0.7	+1.1

the fcc hollow site instead of the top site. However, our calculations show a barrier of about 200 meV to go from the hollow to the top site and less than 100 meV to go from the hollow to the bridge site. In Fig. 4(b) and 4(c), we show the one-dimensional energy landscape for the CO molecule on Cu(211). Two diffusion paths are chosen in this case: (i) top-bridge-top (along the step edge) and (ii) top-fcc-hollow (away from the step). From Fig. 4(b) we conclude that the diffusion of CO from the bridge to the top site is more favorable than that from the top to the hollow site, with a diffusion barrier of about 60 meV for the former compared to about 200 meV for the latter path. These results indicate that CO molecules are more free to roam on the step edge of Cu(211) than away from it.

C. Interlayer relaxations

In Table III, we present a comparison of the interlayer relaxations of the stepped and kinked Cu surfaces as introduced by the adsorption of the CO molecule. The results for the corresponding clean surfaces are also included. The Cu(532) surface has the most dramatic effect of CO adsorption as $\mathbf{d}_{1,2}$, where $\mathbf{d}_{i,j}$ is the vertical separation between layers \mathbf{i} and \mathbf{j} , is found to have a large outward relaxation of +23.5% compared to an inward relaxation of -17.7% for the clean surface. The effect is local and as seen from Table III, there is only a small change in the relaxations for the rest of the layers on CO adsorption. So far no experimental data are available for interlayer relaxation on Cu(532), however, our calculated trend for clean Cu(532) is in agreement with those calculated with many-body potentials.³⁶ On the stepped surface Cu(221), the effect of CO adsorption is also mostly on

$\mathbf{d}_{1,2}$ in which the large inward relaxation of -16.5% on the clean surface is overtaken by a small outward relaxation of +2.9%. Calculated interlayer relaxations on clean Cu(221) match well with those obtained with the full-potential linear augmented plane-wave method (FP-LAPW),³⁷ and with many-body potentials³⁸ for this surface. The calculated interlayer relaxations of clean Cu(221) also agree with those obtained from low-energy electron-diffraction measurements and previous theoretical techniques.^{21,39,40} Like the two above surfaces, results for Cu(211) show that the strong contraction of -15.6% between layers 1 and 2 of the clean surface is overtaken by a small inward relaxation of +6.4% on CO chemisorption. This general trend of the change in the top layer relaxation from a large contraction to expansion upon adsorption of CO is in good accord with the observation by Ibach and Bruchman⁴¹ who reported a surface vibrational mode above the bulk band for the vicinal surface Pt(775) (due to the large contraction) that disappears when CO is adsorbed (reflecting the change of the large contraction to an expansion).

D. Vibrational properties and work functions

Vibrational properties of a “free” CO molecule were calculated by fully relaxing a single molecule in a large super cell of size, approximately, $6 \times 6 \times 22 \text{ \AA}^3$. The stretching mode was calculated to be 264.5 meV. This can be compared with the experimentally measured frequency of isolated CO molecule of 257.8 meV with EELS and of 257.7 meV with infrared (IR) spectroscopy.^{42,43} For the CO-covered Cu surfaces, we have calculated the frequencies of two modes: the metal-molecule ($\nu_{\text{C-Cu}}$) stretch and the intramolecular stretch

TABLE IV. Calculated CO vibrational frequencies on Cu surfaces. $\nu_{\text{C-O}}$ is the CO stretch mode and $\nu_{\text{C-Cu}}$ is metal-C stretch mode. Here “*t*” and “*b*” represent the top and bridge sites (see Fig. 1), respectively.

Surface	Vibrational Frequency (meV)	
	$\nu_{\text{C-Cu}}$	$\nu_{\text{C-O}}$
Cu(211)	251.2 (<i>t</i>)	40.3 (<i>t</i>)
	236.2 (<i>b</i>)	38.4 (<i>b</i>)
Cu(221)	251.0 (<i>t</i>)	40.1 (<i>t</i>)
	235.5 (<i>b</i>)	36.7 (<i>b</i>)
Cu(532)	252.1 (<i>t</i>)	41.0 (<i>t</i>)
	235.7 (b_{KS1})	36.0 (b_{KS1})
	233.9 (b_{KS2})	36.4 (b_{KS2})

($\nu_{\text{C-O}}$). We find a small drop in the vibrational frequency as compared to that of the gas phase CO as a result of the bonding of the CO with the Cu surface atom. The frequencies of the CO vibrational modes calculated for all surfaces are summarized in Table IV. For all cases in which CO is adsorbed on the top site we see almost the same value of the CO stretching frequency ($\nu_{\text{C-O}}$), as expected. However, there is a small increase in $\nu_{\text{C-Cu}}$, with a decrease in the coordination of the substrate atom. This is also to be expected since molecules adsorbed on the low coordinated sites will have stiffer bonds than those on highly coordinated sites. This same explanation holds for our finding of a decrease of about 14–16 meV in the vibrational frequency of the CO stretch mode from on-top to bridge site adsorption. The drop of 2–4 meV for the value of $\nu_{\text{C-Cu}}$ from the top to bridge site is also similarly understood. Our findings are in agreement with the arguments put forward by Ishi *et al.*⁴⁴

In Table V, we have summarized our calculated work functions (ϕ) for all Cu surfaces considered here, with and without the adsorbate, along with available experimental values for clean surfaces of Cu(100), Cu(111), and Cu(110). For these three low Miller index surfaces our results are in qualitative agreement with the experimental data, although our calculated work functions are about 10% smaller than the experimental results.^{45–47} We find a decrease in the work function for clean surfaces with a decrease in the coordination of the surface atoms, as noted by the results in Table V for the low Miller index surfaces. The calculated work functions also show a dependence on the local step geometry. For example, for the two types of vicinals of Cu(111), ϕ decreases by 0.29 and 0.14 eV, respectively, for Cu(211) and

Cu(221) from that for Cu(111). The decrease in the work function ($\Delta\phi$) for the kinked surface Cu(532) from that for Cu(111) is 0.41 eV. Our calculations show a further decrease in the work functions when CO is adsorbed on the surface again in qualitative agreement with the conclusions of Ishi *et al.*⁴⁴ from comparison of various experiments^{33,48,49} that unlike group-VIII elements, all of group IB (Cu, Ag, Au) show this decreasing trend of work functions with CO adsorption.

E. Surface electronic structure

When an electronegative element like C is adsorbed on a metallic surface, it tends to take charges away from the surface. Such charge transfer has understandably a strong dependence upon the coordination of the adsorbate, as reported in many studies.⁵⁰ Since we have considered CO adsorption on a variety of local atomic environments it is important that we examine the differences in the local electronic structure and the nature of the bonding of the CO with the substrate. In Fig. 5, we have plotted the local density of the *d* state (LDOS) of Cu atoms and the *sp* states of C and O atoms to study the *sp-d* hybridization, for the three high Miller index surfaces of interest. First of all, we see narrowing (Fig. 5) of the *d* band for the lower coordinated surfaces, as found by Tersoff and Falicov⁵¹ in their calculations of Ni and Cu surfaces. The *sp* state of C and O are split and have almost filled bonding states, which hybridize with the *d* state of Cu as can be seen from appearance of the features at the same low energies in the LDOS plotted for CO and its neighboring Cu atoms in Fig. 5. This effect is found to be localized on stepped surfaces Cu(211) and Cu(221), for which the LDOS of only the step atom appears to be involved in the hybridization with *sp* bands of CO. On the other hand, in the case of Cu(532), these differences in the hybridization in *sp-d* states of the stepped and kinked surface may provide the rationale for the difference in E_{ad} for CO on the surface even though CO is adsorbed on the top site we see a small redistribution of LDOS for next layer atom, as a result of the small interlayer separation, i.e., 0.296 Å for (532). Earlier studies¹⁰ also show that it is mostly the repulsive interaction of *s* states of CO with substrate which plays a key role in determining the trends in adsorption energies. Our LDOS plots also show that it is mostly 4σ and 5σ (see Fig. 5) states of CO which mainly affect the metal surface as argued in previous calculations for Cu(111).¹³

IV. CONCLUSIONS

In this paper, we have presented the results of a detailed theoretical investigation of CO adsorption on three low

TABLE V. Calculated work function ϕ (in eV) for clean and CO adsorbed Cu surfaces along with the available experimental values from Refs. 43, 45, and 46 in parentheses. The data of $\Delta\phi$ are taken from Refs. 33, 48, and 49.

Surface	Cu(111)	Cu(100)	Cu(110)	Cu(211)	Cu(221)	Cu(532)
Clean	4.89 [4.98 (Ref. 43)]	4.63 [4.65 (Ref. 45)]	4.45 [4.48 (Ref. 46)]	4.60	4.75	4.48
With CO	4.74	4.50	4.28	4.57	4.42	4.41
$\Delta\phi^{\text{exp}}$	-0.47 (Ref. 33)	-0.23 (Ref. 48)	-0.29 (Ref. 49)			

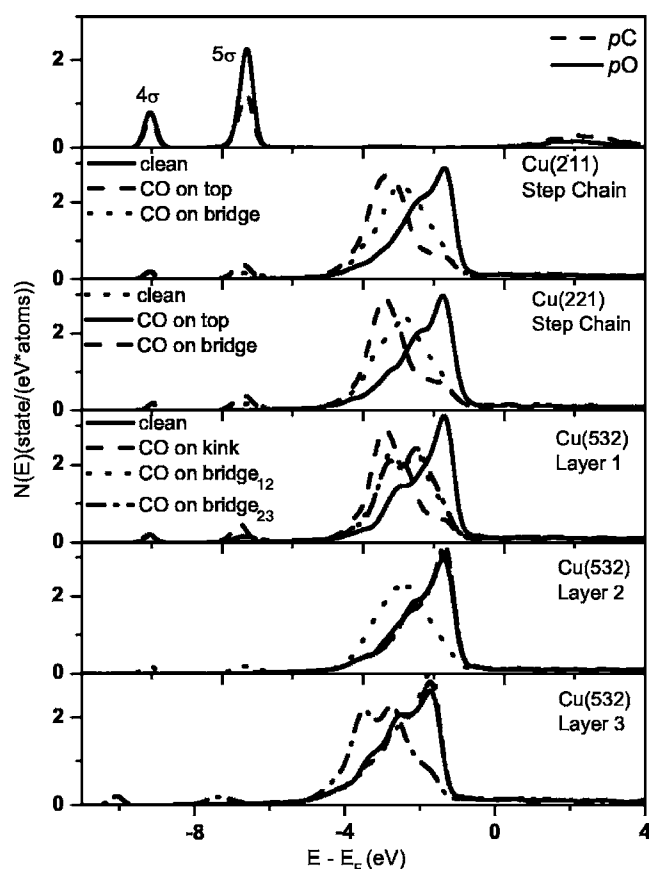


FIG. 5. Local density of state of clean and CO adsorbed Cu surfaces. Top panel shows the p states of CO molecule, the next two panels show the effect of CO on SC [see Fig. 1(d)] of Cu(211) and Cu(221). The last three panels show the top three layers on Cu(532).

Miller index surfaces, namely, (111), (100), (110), two stepped surfaces, (211) and (221), and a kinked (532) surface of Cu. The CO was adsorbed on experimentally observed preferred sites to explain trends in adsorption energies due to different geometrical and chemical structure. We find the adsorption energy for CO to increase with decrease in the local coordination of surface atoms, with the kinked site on Cu(532) with lowest coordination being the most favorable for CO adsorption. On the other hand, the bridge sites of Cu(211) and Cu(221) were found to be slightly preferred over the top site. We also found a strong dependence of adsorption energy on the coverage of the adsorbate: a large decrease in the adsorption energy was found with increase in coverage. Our calculations of the diffusion of the CO molecule on metal surfaces indicate that CO diffuses more easily along the step edge, as compared to away from the step edge (terrace). A very small drop in the vibrational frequency of the free molecule was noted when it was adsorbed on the metal surface but difference within different surfaces was negligible for on-top adsorption. The work function of clean Cu surfaces was also found to be dependent on the local surface geometry, while that on adsorbate covered surface was found to decrease in all cases compared to the clean surface.

ACKNOWLEDGMENTS

The authors would like to thank Sergey Stolbov and Claude R. Henry for interesting and helpful discussions. We also acknowledge financial support from the U.S. Department of Energy under Grant No. DE-FGO2-03ER15465 and computational resources provided by the National Science Foundation Cyberinfrastructure and TeraGrid Grant No. TG-DMR050018N.

¹G. Blyholder, *J. Phys. Chem.* **68**, 2772 (1964).

²P. S. Bagus, C. J. Nelin, and C. W. Bauschlicher, *Phys. Rev. B* **28**, 5423 (1983).

³S. M. Davis and G. A. Somorjai, in *The Chemical Physics of Solid Surfaces*, edited by D. A. King and D. A. Woodruff (Elsevier, Amsterdam, 1982), Vol. 4.

⁴J. C. Campazona, in *The Chemical Properties of Solid Surfaces and Heterogeneous Catalysis*, edited by D. A. King and D. P. Woodruff (Elsevier, Amsterdam, 1990), Vol. 3, Part A.

⁵H. Wagner, in *Springer Tracts in Modern Physics*, edited by G. Hoehler (Springer, Berlin, 1987).

⁶H. Over, *Prog. Surf. Sci.* **58**, 249 (2001).

⁷S. Sung and R. Hoffmann, *Prog. Surf. Sci.* **107**, 578 (1985).

⁸C. R. Henry, *Surf. Sci. Rep.* **31**, 231 (1998).

⁹S. Vollmer, G. Witte, and C. Wöll, *Catal. Lett.* **77**, 97 (2001).

¹⁰P. Bagus and C. Wöll, *Chem. Phys. Lett.* **294**, 599 (1999).

¹¹P. Hohenberg and W. Kohn, *Phys. Rev.* **136**, A864 (1964).

¹²W. Kohn and L. J. Sham, *Phys. Rev.* **140**, A1133 (1965).

¹³M. Gajdos, A. Eichler, and J. Hafner, *J. Phys.: Condens. Matter* **16**, 1141 (2004).

¹⁴F. Favot, A. D. Corso, and A. Baldereschi, *J. Chem. Phys.* **114**,

483 (2001).

¹⁵M. Gajdos and J. Hafner, *Surf. Sci.* **590**, 117 (2005).

¹⁶S. E. Mason, I. Grinberg, and A. M. Rappe, *Phys. Rev. B* **69**, 161401(R) (2004).

¹⁷G. Kresse and J. Hafner, *Phys. Rev. B* **47**, 558 (1993).

¹⁸G. Kresse and J. Furthmüller, *Comput. Mater. Sci.* **6**, 15 (1996).

¹⁹G. Kresse and J. Furthmüller, *Phys. Rev. B* **54**, 11169 (1996).

²⁰D. Vanderbilt, *Phys. Rev. B* **41**, 7892 (1990).

²¹M. Gajdos, A. Eichler, J. Hafner, G. Meyer, and K-H. Rieder, *Phys. Rev. B* **71**, 035402 (2005).

²²J. P. Perdew, J. A. Chevary, S. H. Vosko, K. A. Jackson, M. R. Pederson, D. J. Singh, and C. Fiolhais, *Phys. Rev. B* **46**, 6671 (1992).

²³P. Fouquet, R. A. Olsen, and E. J. Baerends, *J. Chem. Phys.* **119**, 509 (2003).

²⁴H. J. Monkhorst and J. D. Pack, *Phys. Rev. B* **13**, 5188 (1976).

²⁵J. Braun, A. P. Graham, F. Hofmann, W. Silvestri, J. P. Toennies, and G. Witte, *J. Chem. Phys.* **105**, 3258 (1996).

²⁶A. P. Graham, F. Hofmann, J. P. Toennies, G. P. Williams, C. J. Hirschmugl, and J. Ellis, *J. Chem. Phys.* **108**, 7825 (1998).

²⁷S. Stolbov, F. Mehmood, T. S. Rahman, M. Alatalo, I. Makkonen,

- and P. Salo, *Phys. Rev. B* **70**, 155410 (2004).
- ²⁸E. J. Moler, S. A. Kellar, W. R. A. Huff, Z. Hussain, Y. Chen, and D. A. Shirley, *Phys. Rev. B* **54**, 10862 (1996).
- ²⁹S. Andersson and J. B. Pendry, *Phys. Rev. Lett.* **43**, 363 (1979).
- ³⁰C. F. McConville, D. P. Woodruff, K. C. Prince, G. Paolucci, V. Chab, M. Surman, and A. M. Bradshaw, *Surf. Sci.* **166**, 221 (1986).
- ³¹S. Y. Liem and J. H. R. Clarke, *J. Chem. Phys.* **121**, 4339 (2004).
- ³²A. Föhlisch, W. Wurth, M. Stichler, C. Keller, and A. Nilsson, *J. Chem. Phys.* **121**, 4848 (2004).
- ³³J. C. Tracy, *J. Chem. Phys.* **56**, 2748 (1972).
- ³⁴L. D. Peterson and S. D. Kevan, *Surf. Sci. Lett.* **235**, L285 (1990).
- ³⁵C. M. Truong, J. A. Rodriguez, and D. W. Goodman, *Surf. Sci. Lett.* **271**, L385 (1992).
- ³⁶F. Mehmood, A. Kara, and T. S. Rahman, *Surf. Sci.* **600**, 4501 (2006).
- ³⁷J. L. F. Da Silva, K. Schroeder, and S. Blügel, *Phys. Rev. B* **70**, 245432 (2004).
- ³⁸I. Y. Sklyadneva, G. G. Rusina, and E. V. Chulkov, *Surf. Sci.* **416**, 17 (1998).
- ³⁹S. Durukanoglu, A. Kara, and T. S. Rahman, *Phys. Rev. B* **55**, 13894 (1997).
- ⁴⁰T. Seyller, R. D. Diehl, and F. Jona, *J. Vac. Sci. Technol. A* **17**, 1635 (1999).
- ⁴¹H. Ibach and D. Bruchmann, *Phys. Rev. Lett.* **41**, 958 (1978).
- ⁴²C. J. Hirschmugl, G. P. Williams, F. M. Hoffmann, and Y. J. Chabal, *Phys. Rev. Lett.* **65**, 480 (1990).
- ⁴³R. Raval, S. F. Parker, M. E. Pemble, P. Hollins, J. Pritchard, and M. A. Chesters, *Surf. Sci.* **203**, 353 (1988).
- ⁴⁴S. Ishi, Y. Ohno, and B. Viswanathan, *Surf. Sci.* **161**, 349 (1985).
- ⁴⁵C. J. Fall, N. Binggeli, and A. Baldereschi, *Phys. Rev. B* **61**, 8489 (2000).
- ⁴⁶R. Arafune, K. Hayashi, S. Ueda, and S. Ushioda, *Phys. Rev. Lett.* **92**, 247601 (2004).
- ⁴⁷W. Mantz, James K. G. Watson, K. Narahari Rao, D. L. Albritton, A. L. Schmeltekopf, and R. N. Zare, *J. Mol. Spectrosc.* **39**, 180 (1971).
- ⁴⁸P. Hollins and J. Pritchard, *Surf. Sci.* **89**, 486 (1979).
- ⁴⁹K. Horn, M. Hussain, and J. Pritchard, *Surf. Sci.* **63**, 244 (1977).
- ⁵⁰A. Föhlisch, M. Nyberg, J. Hasselström, O. Karis, L. G. M. Pettersson, and A. Nilsson, *Phys. Rev. Lett.* **85**, 3309 (2000).
- ⁵¹J. Tersoff and L. M. Falicov, *Phys. Rev. B* **24**, 754 (1981).